GLOBAL JOURNAL OF PHARMACEUTICAL AND SCIENTIFIC RESEARCH
(GJPSR)

Volume-1, Issue-3, October- 2025

Article Received on 02/10/2025 Article Revised on 11/10/2025 Article Accepted on 29/10/2025

DEVELOPMENT AND EVALUATION OF SUBMICRON LIPID NANOPARTICLES FOR THE ORAL DELIVERY OF PACLITAXEL

Mansram Alke[1], Praveen Bhawsar[2], Praveen Kumar Jain[3], Sheenam mansuri[4]

[1]Scholar, Malhotra College of Pharmacy, Bhopal, Madhya Pradesh

[2]Associate Professor, Malhotra College of Pharmacy, Bhopal, Madhya Pradesh

[3]Professor, Malhotra College of Pharmacy, Bhopal, Madhya Pradesh

[4]Associate Professor, Malhotra College of Pharmacy, Bhopal, Madhya Pradesh

Corresponding Author: Mansram Alke

Abstract:

Paclitaxel is a potent anticancer drug, but its oral application is severely limited by low aqueous solubility, gastrointestinal degradation, and extensive first-pass metabolism. This study developed and optimized paclitaxel-loaded solid lipid nanoparticles (SLNs) using microemulsion and modified solvent injection techniques to enhance oral bioavailability and systemic exposure. Comprehensive characterization by DLS, SEM, TEM, DSC, and FTIR confirmed uniform spherical morphology, high encapsulation efficiency, and molecular dispersion of the drug without crystalline residues. Stability assessments at 4°C and 25°C demonstrated preserved particle integrity and drug content over the study period. In vivo pharmacokinetic evaluation in mice revealed markedly increased plasma concentrations, prolonged half-life, and nearly a 10-fold enhancement in AUC compared to free paclitaxel. Tissue distribution profiles showed improved uptake in liver, kidney, spleen, and brain, indicating reduced first-pass metabolism and enhanced systemic transport. No significant hematological, biochemical, or histopathological alterations were observed, confirming biocompatibility. Overall, SLNs provide a promising and safe oral delivery strategy for improving therapeutic efficacy and absorption of paclitaxel in cancer treatment.

Keywords: Paclitaxel; Solid Lipid Nanoparticles (SLN); Oral bioavailability; Modified solvent injection

1. Introduction

Paclitaxel is an important chemotherapeutic agent used extensively in the treatment of solid tumors such as breast, ovarian, and lung cancers (Rowinsky & Donehower, 1995). However, its clinical utility is restricted by extremely low aqueous solubility, extensive first-pass metabolism, and poor oral absorption, necessitating the use of intravenous formulations that contain Cremophor EL, a solvent associated with hypersensitivity reactions and dose-limiting toxicities (Weiss et al., 1990; Gelderblom et al., 2001). As a result, there is significant interest in developing alternative delivery systems capable of improving the oral bioavailability and safety profile of paclitaxel.

Solid Lipid Nanoparticles (SLNs) offer several advantages for oral delivery, including biocompatibility, improved solubility of lipophilic drugs, protection from gastrointestinal degradation, controlled release, and enhanced lymphatic transport (Müller et al., 2000; Mehnert & Mäder, 2001). Their small particle size and solid lipid matrix enable prolonged systemic circulation and reduced first-pass metabolism, making them attractive carriers for drugs like paclitaxel. Previous studies have shown improved oral absorption of other anticancer and poorly soluble compounds when formulated into SLNs (Zur Mühlen et al., 1998; Cavalli et al., 2000).

Despite these advantages, the performance of SLNs is critically dependent on formulation variables, lipid–surfactant interactions, and manufacturing methods. Techniques such as microemulsion and solvent injection have been widely explored, but their reproducibility, particle size distribution, and drug loading efficiency vary significantly (Gasco, 1997; Schubert & Goymann, 2003). Therefore, systematic optimization and characterization are essential to obtain SLNs with desirable physicochemical and biological properties.

The present study focuses on the development of paclitaxel-loaded SLNs using microemulsion and modified solvent injection techniques, followed by comprehensive characterization using DLS, SEM, TEM, DSC, and FTIR to evaluate particle size, morphology, thermal properties, and drug–excipient compatibility. A sensitive HPLC method was validated for accurate quantification of paclitaxel in biological matrices. Furthermore, pharmacokinetic, biodistribution, and toxicity studies in mice were performed to determine whether the optimized SLN formulation could enhance oral absorption, prolong systemic exposure, and

maintain safety. These investigations aim to establish SLNs as a promising and efficient platform for oral paclitaxel delivery.

2. MATERIAL AND METHOD

2.1 Preparation Of Standard Solutions/Buffers

2.1.1 Simulated gastric fluid

Dissolved 2.0 g of sodium chloride and 3.2g of pepsin in 7.0 ml of hydrochloric acid and added sufficient water to make 1000 ml. This test solution had a pH of about 1.2. (USP XXIV, pH 1.2, pepsin 0.32% w/v).

2.1.2 Phosphate buffered saline (FIBS) pH 7,4

PBS pH 7.4 was prepared as per raetliod given in IP, 1985. 1.38 g of disodiiini liydrogen phosphate, 0.19 g of potassium dihydrogen phosphate and 8.0 g of sodium chloride were dissolved in sufficient water to produce 1000 ml. Immediately before use the pH was adjusted, if necessary.

2.2 CHARACTERIZATION AND IDENTIFICATION OF PACLITAXEL

Paclitaxel was evaluated based on its physical properties such as color and solubility. Its identity was confirmed using melting point determination, UV spectroscopy, X-ray diffraction, and FTIR analysis, which were compared with a reference standard.

2.3 ANALYTICAL METHODOLOGY FOR PACLITAXEL

Paclitaxel was analyzed using a sensitive HPLC method equipped with UV detection to ensure accurate quantification.

2.3.1 Instrumentation

Paclitaxel analysis was performed using a Thermo Finnigan LC Surveyor HPLC system comprising a quaternary pump, autosampler with 100 µL loop, and a degasser. Detection was carried out using a Surveyor PDA detector, and data processing was done with Chromquest software.

2.3.2 Chromatographic conditions

Paclitaxel was analyzed using a LiChroCART® 250-4 LiChrospher® 100 RP-18 column (5 µm) with a matching guard column. The mobile phase was ACN:water (70:30), filtered (0.22 µm) and degassed. The flow rate was 1 mL/min at 25 ± 1°C, with UV detection at 227 nm and a 20 µL injection volume. Data acquisition was performed using Chromquest software (Crosasso et al., 2000; Chen et al., 2001).

2.4 PREPARATION OF SOLID LIPID NANOPARTICLES

2.4.1 Preparation of SLN using established Micro emulsion technique

SLNs were prepared using Gasco's microemulsion method (Gasco, 1997; Bocca et al., 1998; Tiyaboonchai et al., 2007). Melted lipid (75°C) was mixed with a water-surfactant solution at the same temperature, then added to cold water (2–3°C, 1:10) to form SLNs. The dispersion was ultracentrifuged (40,000 g, 1 h, 4°C), redispersed in trehalose, freeze-dried, and resuspended before evaluation. Particle size, zeta potential, and morphology were analyzed using PCS and SEM (Cavalli et al., 2000; Heydenreich et al., 2003).

2.4.2. Preparation of SLN using modified solvent injection technique

SLNs were prepared by dissolving lipid and soya lecithin in ether and rapidly injecting the solution into water (40 ± 2°C) under stirring, followed by homogenization (20,000 rpm, 1 h). After solvent evaporation (30°C, 30 min), the dispersion was ultracentrifuged (40,000 g, 1 h, 4°C), redispersed in trehalose, freeze-dried (24 h), and resuspended before evaluation (Schubert & Goymann, 2003; Cavalli et al., 2000; Heydenreich et al., 2003).

2.5 OPTIMIZATION PARAMETERS FOR MODIFIED SOLVENT INJECTION TECHNIQUE

The SLN preparation was optimized by varying solvent injection volume (0.5–10 mL), homogenization speed (15,000–25,000 rpm), lipid concentration (0.12–0.92 mmol), and poloxamer 188 concentration (0.1–2.0% w/v) (Ahlin et al., 1998; Schubert and Goymann, 2003). Dispersions were characterized for particle size, zeta potential, and morphology using SEM and PCS.

2.6 PREPARATION OF PACILTAXEL LOADED SLN USING MODIFIED SOLVENT INJECTION METHOD

Paclitaxel-loaded SLNs were prepared by adding different drug loads (0.05, 0.25, and 0.5 mmol) dissolved in dichloromethane (DCM) to an ether solution containing lipid (0.23 mmol), soya lecithin (0.175 mmol), and α-tocopherol (0.025 mmol) (Ceruti et al., 2000; Xu et al., 2005; Tauhari and Dash, 2006). The subsequent steps followed the same procedure as for blank SLN fabrication.

2.7 CHARACTERIZATION OF SOLID LIPID NANOPARTICLES

Blank and paclitaxel-loaded SLNs prepared by microemulsion and modified solvent injection methods were characterized using advanced techniques to evaluate their properties (Schwarz et al., 1994; Cavalli et al., 2000; Fonseca et al., 2002; Dong and Feng, 2004; Lee et al., 2007).

2.7.1 Surface Morphology

The surface morphology of drug free and drug loaded SLN were investigated by scanning electron microscopy (SEM) and transmission electron microscopy (TEM).

2.7.1.1. Scanning Electron Microscopy (SEM)

SLN samples were dried using a critical point dryer, gold-coated under argon (SCD 020), and imaged at 15 kV using a LEO 435 VP SEM. The electron beam (0.4–5 nm spot) interacts with the sample to emit electrons and radiation, forming high-resolution images (Mu and Feng, 2001; Dubes et al., 2003).

2.7.1.2. Transmission Electron Microscopy (TEM)

SLN dispersions were diluted, stained with 2% sodium phosphotungstic acid, and placed on copper grids for imaging. TEM analysis was performed using an FEI Morgagni 268D at 80 kV with magnification up to 220,000× to observe particle morphology (Cavalli et al., 2000; Fonseca et al., 2002; Straub et al., 2005).

2.7.2 Size and Zeta Potential Measurements

Particle size and zeta potential of blank and drug-loaded SLNs were measured using a Zetasizer Nano ZS90 (Malvern, UK) at 25°C. Size was determined by DLS and reported as z-average and PDI, while zeta potential was calculated from electrophoretic mobility. Samples were diluted in particle-free water and analyzed in triplicate, with results expressed as median ± range (Freitas & Müller, 1999; Cavalli et al., 2000; Feng & Huang, 2001).

2.7.3 Differential scanning calorimetry (DSC)

DSC thermograms of paclitaxel, lipids (stearic acid, stearylamine), drug-lipid mixtures, and drug-loaded SLNs were recorded using a Perkin Elmer Pyris 6 DSC with 5 mg samples in aluminum pans. Scans were performed at 10°C/min over 35–100°C for lipids and 35–300°C for drugs and mixtures under nitrogen. Drug physical state was assessed by its melting point on the DSC curve (Mu and Feng, 2001; Dhanikula and Panchagnula, 2004; Xie et al., 2005).

2.8 *IN VIVO* STUDIES

2.8.1 Preparation of SLN for *in vivo* studies

Paclitaxel-loaded SLNs for oral administration were prepared at a dose of 40 mg/kg. The required drug amount was calculated as (drug per animal ÷ mean incorporation efficiency) × 100, and equivalent lipid was added. SLNs were then fabricated using the previously described method (Kim et al., 2001; Taraboletti et al., 2005).

2.8.2 Pharmacokinetics and biodistribution studies

Animals

Pharmacokinetic and biodistribution studies were performed in male Swiss albino mice (~50 g) from the Central Experimental Animal Facility, AIIMS, New Delhi (IAEC no. 360/IAEC/06). Mice were housed five per cage with ad libitum access to food and water, maintained according to AIIMS animal care guidelines.

Dosing Solutions

A 6 mg/mL paclitaxel stock solution was prepared in ethanol and polysorbate 80, stable at 4°C for 1 year; for i.v. use, it was diluted to 1 mg/mL (Crofton et al., 1995; Bardelmeijer et al., 2000). Oral SLN formulations were freshly suspended in water, sonicated, and stirred to 0.8 mg/mL, protected from light.

Administration Routes

Oral doses of free drug and SLN formulations were given by gavage, while i.v. administration was via lateral tail vein injection using a 29-gauge needle. Animals were warmed under a heating lamp, and no anesthesia was used.

Groups

Studies were approved by the AIIMS Institutional Animal Care and Use Committee. Mice were randomly divided into three groups: Group A – oral paclitaxel, Group B – oral paclitaxel-loaded SLN, Group C – i.v. paclitaxel. Oral dose was 40 mg/kg (Groups A & B) and i.v. dose 10 mg/kg (Group C). Animals were fasted 12 h before dosing, with water ad libitum. Blood samples were collected at defined time points: Groups A & B – 0, 0.25, 0.5, 1, 2, 4, 6, 24 h; Group C – 0.08, 0.25, 0.5, 1, 2, 4, 6, 8, 12 h, with 5 animals per time point for oral and 3 for i.v. administration (Sparreboom et al., 1997; Ceruti et al., 2000; Bardelmeijer et al., 2000; Xu et al., 2005).

Sample Collection and Handling

Following treatment, animals were sacrificed under isoflurane anesthesia by cardiac exsanguination. Blood was collected in EDTA tubes, centrifuged (5 min, 5000 rpm) to obtain plasma, and stored at -20°C. Liver, spleen, kidney, lungs, and brain were excised, frozen in liquid nitrogen, and stored at -80°C for organ distribution studies. No survival surgery was performed, and carcasses were incinerated at AIIMS.

2.9 TOXICITY STUDIES

Mice (n=8 per group) were randomized into three groups: Group 1 – oral paclitaxel, Group 2 – drug-free SLN, and Group 3 – paclitaxel-loaded SLN (40 mg/kg). After 15 days, animals were sacrificed under anesthesia, and blood was collected for hematological and liver function tests. Major organs (liver, lungs, kidney, spleen, brain) were fixed in 10% formalin, washed with saline, and processed for histopathological analysis to assess acute toxicity.

Gross Changes: Color changes or the development of any patch was observed.

Histopathological Changes:

Tissues from mice treated with paclitaxel-loaded SLN were dehydrated through graded alcohols (70–100%), cleared with xylene, and embedded in paraffin. Thin sections (3–5 µm) were cut using a rotary microtome, deparaffinized, rehydrated through graded alcohols (100–73%), and stained with hematoxylin and eosin for microscopic examination. Sections from drug-free SLN and orally administered paclitaxel were similarly processed as controls.

3. RESULTS AND DISCUSSION

3.1 CHARACTERIZATION AND IDENTIFICATION OF PACLITAXEL

3.1.1 Physical characteristics

Test	USP Specification	Result
Description	A white to off-white powder	White powder
Solubility	Practically insoluble in water, Complies easily soluble in methanol, chloroform, ethyl ether and ethanol	

3.1.2 UV Absorption Spectroscopy

The UV absorption spectrum of paclitaxel in acetonitrile showed a clear λ_max at 227 nm, consistent with previously reported spectral data. This strong correlation with reference values confirms the purity and identity of the paclitaxel sample.

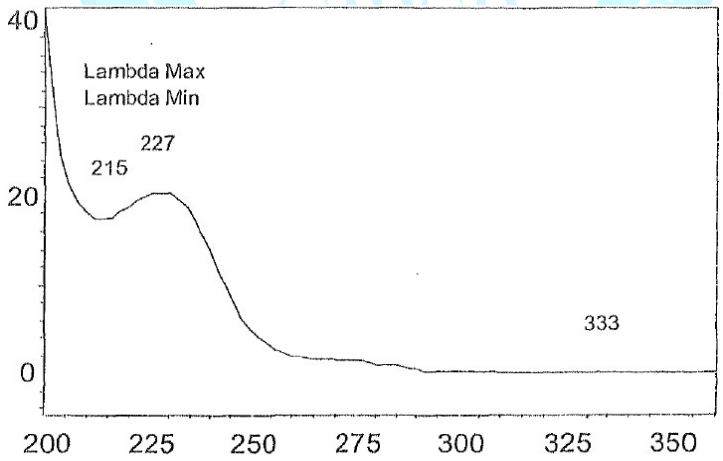

Figure 5-2. U V Spectra of Paclitaxel

3.1.3 Determination of Melting Point

The melting point of paclitaxel was determined using DSC (Model DSC6, Perkin Elmer) under a nitrogen atmosphere with a heating rate of 10°C/min, yielding a value of 219.59°C. This

result closely matched previously reported values, confirming the identity and purity of the sample (Mu and Feng, 2001; Zhang et al., 2004; Dhanikula and Panchagnula, 2004).

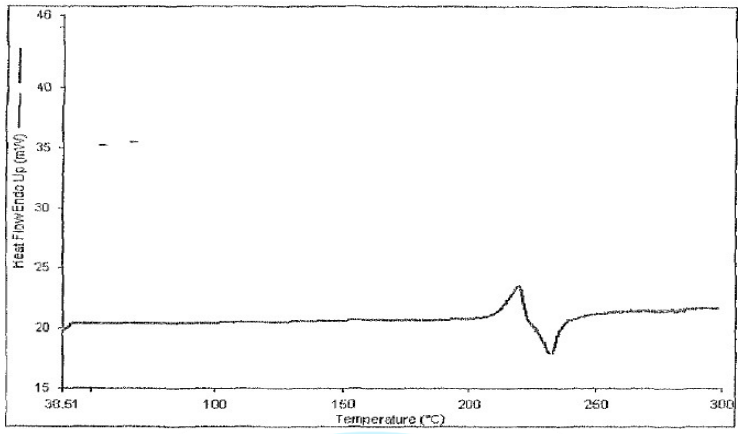

Figure 5-3. DSC thermogram of Paclitaxel

3.1.4 X-ray Diffraction

The XRD pattern of the paclitaxel sample was recorded from 3° to 40° 2θ with a 0.050° step size and 2-second counting time per step. The resulting diffraction profile matched previously reported spectra, confirming the sample's authenticity (Dhanikula and Panchagnula, 2004).

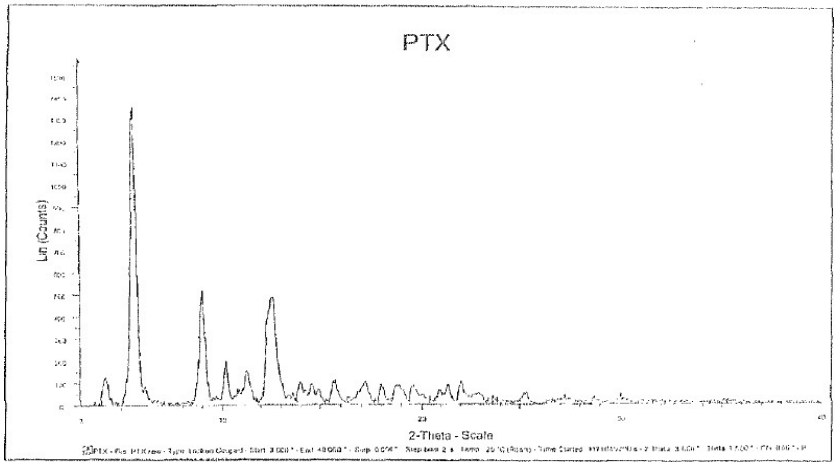

Figure 5-4. X-Ray diffraction pattern of paclitaxel

3.2 ANALYTICAL METHODOLOGY FOR PACLITAXEL

3.2.1 Chromatography

Despite strong UV absorbance at 227 nm (ε = 29,800, methanol) (The Merck Index, 1989), paclitaxel analysis in biological matrices is challenging. A sensitive HPLC method was developed using a 25 cm C18 column and optimized mobile phase, with sample cleanup via solid-phase extraction (SPE) after conventional liquid–liquid extraction proved inadequate. Paclitaxel showed a retention time of ~3.3 min with no endogenous interference, and peak purity was confirmed by photodiode array scanning (Lee et al., 1999; Wang et al., 2003).

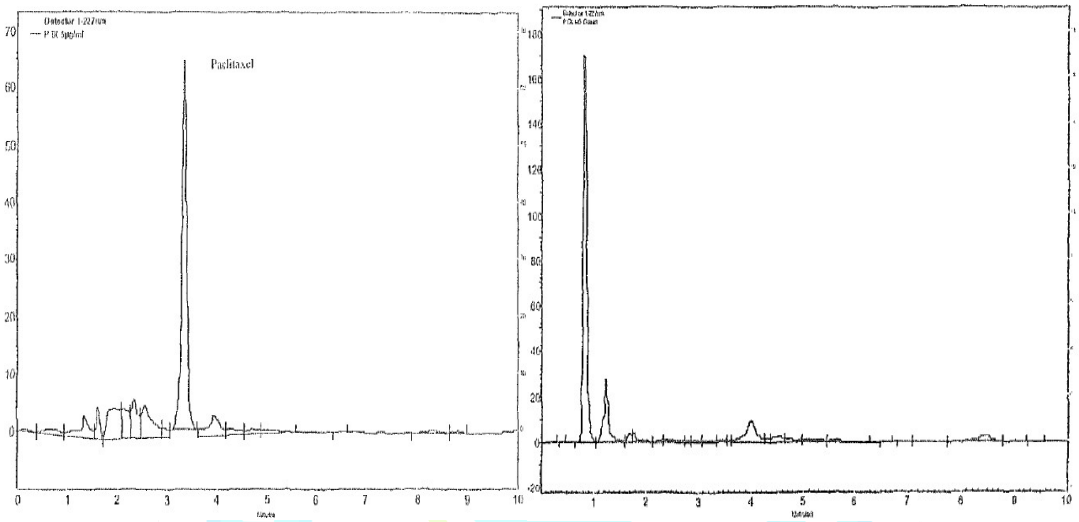

Figure 5-5. Representative chromatogram of paclitaxel standard working solution in 50% ACN

Figure 5-6. Representative chromatogram of extracted blank buffer

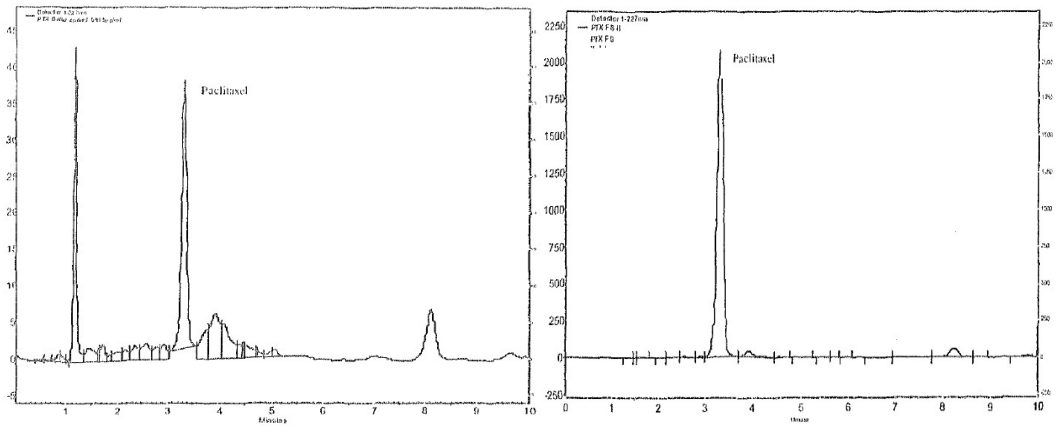

Figure 5-7. Representative chromatogram of buffer spiked with paclitaxel 3.3µg/ml.

Figure 5-8. Representative chromatogram of in *vitro* sample obtained after 6h

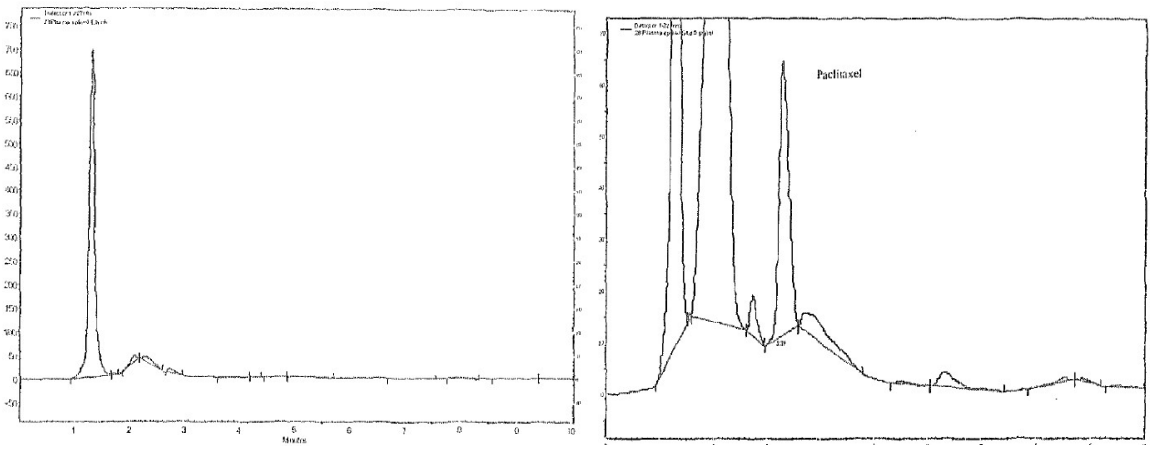

Figure 5-9. Representative chromatogram of extracted blank mouse plasma

Figure 5-10. Representative chromatogram of plasma spiked with paclitaxel! 5µg/ml

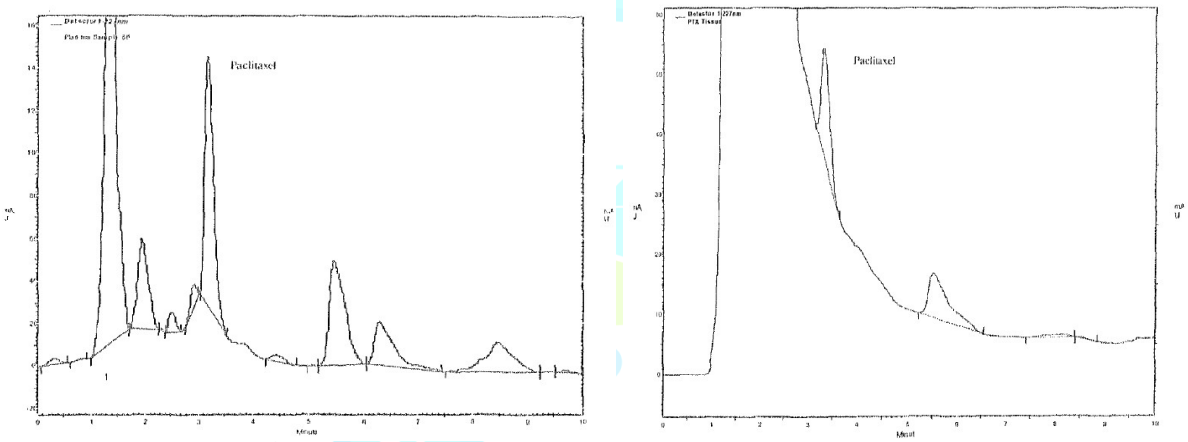

Figure 5-11. Representative chromatogram of plasma sample obtained 6h after a 40mg/kg oral dose of paclitaxel loaded SLN

Figure 5-12. Representative chromatogram of liver sample obtained 6h after a 40mg/kg oral dose of paclitaxel loaded SLN

Linearity

Calibration curves showed excellent linearity. In buffer, linearity was observed from 66–66,666 ng/mL with the equation $y = 149.65x + 995.6$ and $r^2 = 0.9998$ ($n = 3$). In plasma, linearity ranged from 25–20,000 ng/mL, described by $y = 137.08x + 1169$, with an average $r^2 = 0.9999$ ($n = 3$).

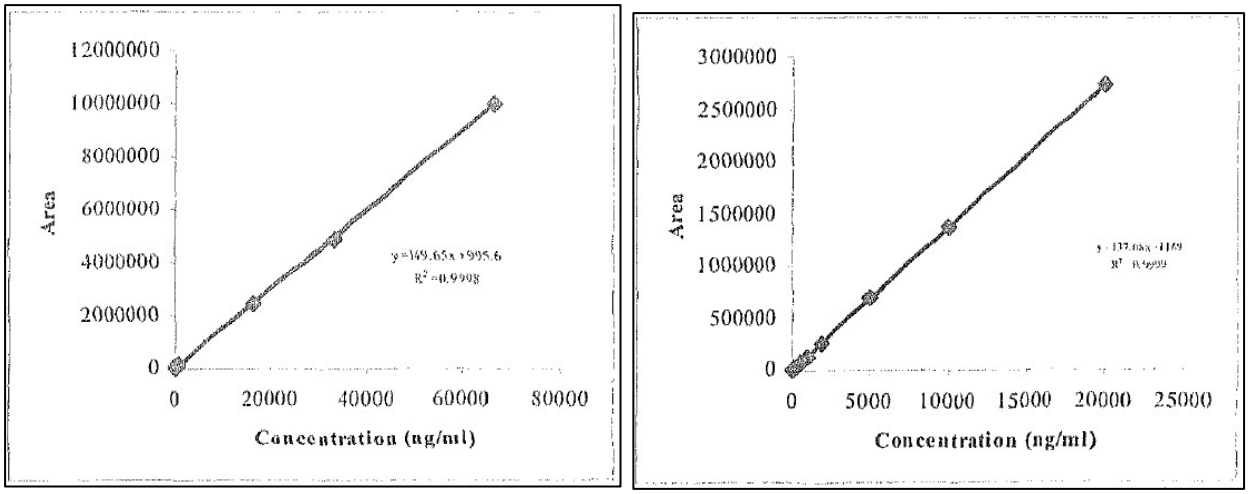

(a) (b)

Figure 5-13. Representative Calibration Curve of Paclitaxel (a) in buffer and, (b) in mouse plasma

Recovery

Paclitaxel recovery was determined by comparing peak areas of extracted samples with unextracted standards. Mean recovery (±SD, n = 3) was 90% in buffer at concentrations 0.066, 1.66, and 6.66 µg/mL. After SPE, plasma recoveries at 0.025, 1, and 10 µg/mL averaged 94%, indicating efficient extraction (Table 5-1).

Table 5-1. Extraction recovery of paclitaxel (mean ±S.D., n=3)

Concentration (µg/ml)	**Recovery (%)**
From buffer	
0.066	89±1.3
1.66	90±1.1
6.66	90±1.6
Mean	90
From mouse plasma	
0.025	87±1.5
1	93±0.7
10	96±1.6

Mean	92

Quantitation limits

The assay showed LOD values of 33 ng/mL (buffer) and 10 ng/mL (plasma). The LOQ, defined as the lowest concentration quantifiable with <20% precision and accuracy error, was 66 ng/mL for buffer and 25 ng/mL for plasma.

Intra- and inter-assay variabilities

Accuracy and precision were evaluated using QC samples at three concentrations analyzed in triplicate. Intraday precision was assessed by three repeated analyses on the same day, while interday precision was determined over three consecutive days. The corresponding accuracy and %RSD precision values are summarized in Table 5-2.

Specificity

Specificity was confirmed by comparing chromatograms of paclitaxel with spiked lipid matrix samples. No interfering peaks were observed, and peak purity across 200–400 nm by photodiode array detection confirmed selective and accurate analyte measurement.

Table 5-2. Intra-day and inter-day accuracy and precision of paclitaxel assay in mouse plasma and buffer

Concentration (µg/ml)	**Intra-day (n=3)**		**Inter day (n=3)**	
Plasma	**Accuracy (%)**	**Precision (%RSD)**	**Accuracy (%)**	**Precision (%RSD)**
0.025	97.1	2.2	95.3	7.8
1	98.5	1.2	97.6	2.7
10	98.0	1.4	96.6	4.6
Buffer				
0.066	94.3	8.9	91.5	13.9
1.66	94.9	3.1	92.6	8.1
6.66	93.4	4.6	92.9	6.3

3.3 ASSESSMENT OF PREPARATION TECHNIQUES

3.3.1 Microemulsion technique

SLNs were prepared via a modified microemulsion method (Bocca et al., 1998) using stearic acid/tripalmitin, soya lecithin, and sodium taurocholate or glycocholate. SLNT averaged 110 ± 3 nm (PDI 0.301 ± 0.02) and SLNG 153 ± 11 nm (PDI 0.242 ± 0.05). Particle size and morphology were analyzed by Zetasizer and SEM.

Table 5-3. Effect of co-surfactant selection on particle size and polydispersity index of SLN (mean ± S.D., n=3)

Sample Code	Co-surfactants	Particle size (nm)	Polydispersity Index
SLNT	Sodium taurocholate	110±3	0.301±0.02
SLNG	Sodium glycocholate	153±11	0.242±0.05

A stearic acid o/w emulsion requires a system HLB of 15. Although sodium glycocholate is more hydrophilic and expected to yield smaller particles, larger particles were observed. Sodium taurocholate, with higher aggregation and better spacing between lecithin head groups, reduces interfacial tension and produces smaller particles. Thus, it was selected as the co-surfactant (Holmberg, 1998).

3.3.1.1 Effect of lipids and surfactants

In microemulsions, droplets are stabilized by a surfactant–co-surfactant interfacial film forming oil, water, and interphase (Attwood, 1994). The effects of lipid type, surfactant-to-lipid ratio, and surfactant-to-co-surfactant ratio on nanoparticle size and stability were studied. The soya lecithin-to-sodium taurocholate molar ratio was varied from 1:4 to 4:1, and the total surfactant-to-lipid ratio from 0.25 to 2.25.

Table 5-4. Effect of different stearic acid, surfactant and co-surfactant molar ratios on particle size and polydispersity index of SLN (mean ± S.D., n=3)

Surfactant: stearic acid	Lecithin: taurocholate	Particle size (nm)	Polydispersity Index
1:4	4:1	440 ± 14.74	0.324 ±0.01
1:1	4:1	241 ± 15.8	0.272 ±0.01
1:0.4	4:1	111 ±10.73	0.222 ± 0.02
1:4	1:4	600 ± 19.06	0.369 ± 0.08
1:1	1:4	380 ± 16.32	0.217 ±0.02
1:0.4	1:4	261 ± 14.41	0.205 ± 0.04

Measurements were performed in triplicate at room temperature. Fatty acids produced smaller nanoparticles than triglycerides. A 4:1 lecithin-to-sodium taurocholate ratio improved particle quality and reduced size, as the anionic co-surfactant lowered interfacial tension, increased negative surface charge, and formed a stable liquid crystalline phospholipid interface.

Table 5-5. Effect of different tripalmitin, surfactant and co-surfactant molar ratios on particle size and polydispersity index of SLN (mean ± S.D., n=3)

Surfactant: tripalmitin	Lecithin: taurocholate	Particle size (nm)	Polydispersity Index
1:4	4:1	700±50.19	0.352 ± 0.05
1:1	4:1	360 ±19.23	0.229 ± 0.02
1:0.4	4:1	310 ± 12.11	0.055 ± 0.03
1:4	1:4	975 ±41.08	0.201 ± 0.09
1:1	1:4	641 ±29.81	0.234 ± 0.06
1:0.4	1:4	450 ± 28.74	0.233 ± 0.02

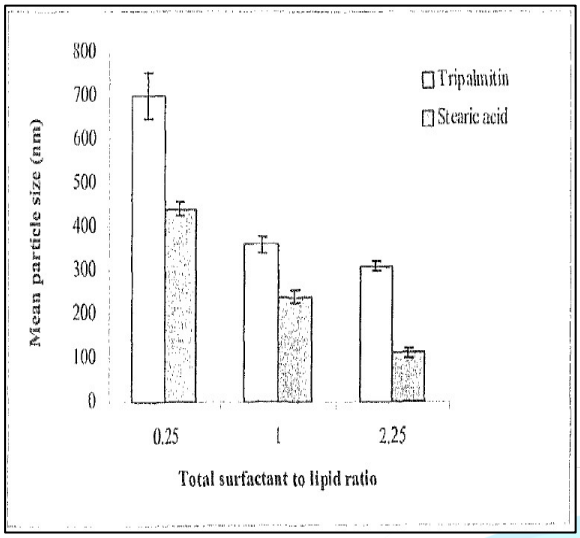

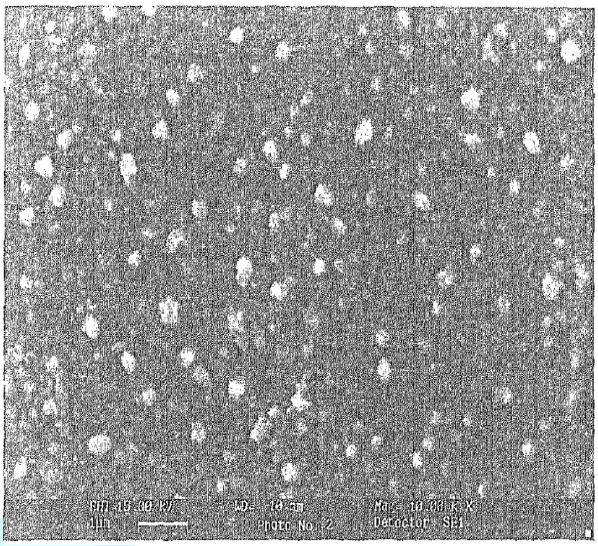

Figure 5-14. Effect of tripalmitin and stearic acid on particle size of SLN (n~3)

Figure 5-15. SEM images of drug free SLN prepared by microemulsion technique

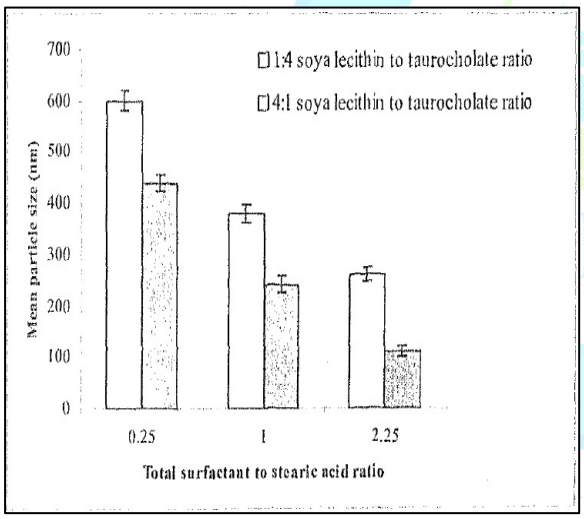

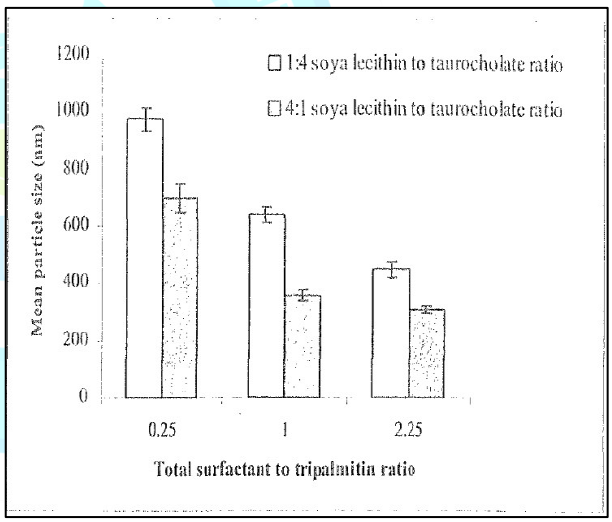

Figure 5-16. Effect of total surfactant to stearic acid ratio on particle size of SLN (n=3)

Figure 5-17. Effect of total surfactant to tripalmitin ratio on particle size of SLN (n-3)

The microemulsion method was abandoned due to poor reproducibility, sensitivity to minor changes, and instability during solidification. Tripalmitin formed tightly packed lattices, limiting paclitaxel incorporation and producing larger particles, so it was not used further (Westesen et al., 1997).

3.3.2 Modified solvent: Injection technique

SLNs were formed by rapidly injecting lipids in diethyl ether into an aqueous phase, avoiding high temperatures, pressures, and toxic solvents. This method allows easy handling, rapid production, and use of pharmaceutically acceptable solvents (Batzri & Korn, 1973; Fessi et al., 1992; Schubert & Goymann, 2003).

Table 5-6. Influence of different lecithin concentrations on the particle size and polydispersity of lipid nanoparticles (mean ± S.D., n==3)

Sample	Lipid (mmol)	Soya Lecithin (mmol)	Mean particle Size (nm)	Polydispersity Index
SLN-L1	0 .1 2	0.02	560 ± 15.3	0.151 ±0.07
SLN-L2	0 .1 2	0.04	395 ± 18.0	0.167 ±0.01
SLN-L3	0 .1 2	0.09	312 ±3.5	0.179 ±0.06
SLN-L4	0 .1 2	0.18	191 ±6.4	0.202 ± 0.02
SLN-L5	0 .1 2	0.35	205 ± 6.4	0.348 ± 0.09

3.4 CHARACTERIZATION OF PACLITAXEL LOADED SLN

3.4.1 Surface Morphology Characterization of paclitaxel-loaded SLN

TEM analysis showed that paclitaxel-loaded SLNs were spherical with a narrow size distribution, consistent with DLS results (Table 5-9). No large aggregates (>170 nm) were observed, indicating the absence of microprecipitates.

3.4.2 Surface Charge Characterization

The zeta potential of the paclitaxel-loaded SLNs, summarized in Table 5-9, indicated sufficient surface charge for stability. Values were within the range (>30 mV) required for full electrostatic stabilization (Schwarz et al., 1994).

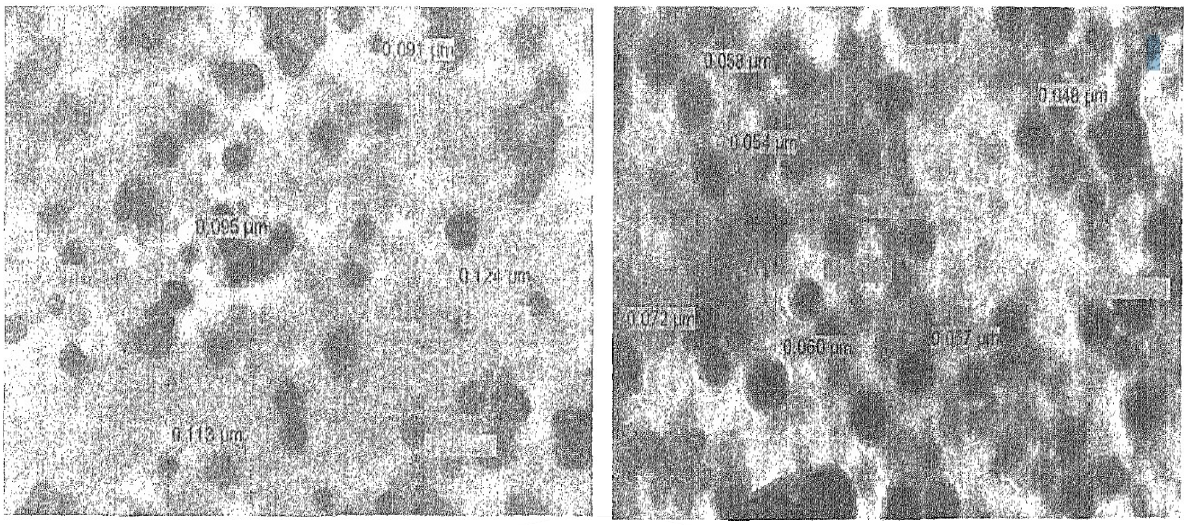

Figure 5-25. TEM images of Paclitaxel loaded stearic acid – SLN (1.5% w/v poloxamer)

Figure 5-26. TEM images of Paclitaxel loaded stearyl amine – SLN (1.5% w/v poloxamer)

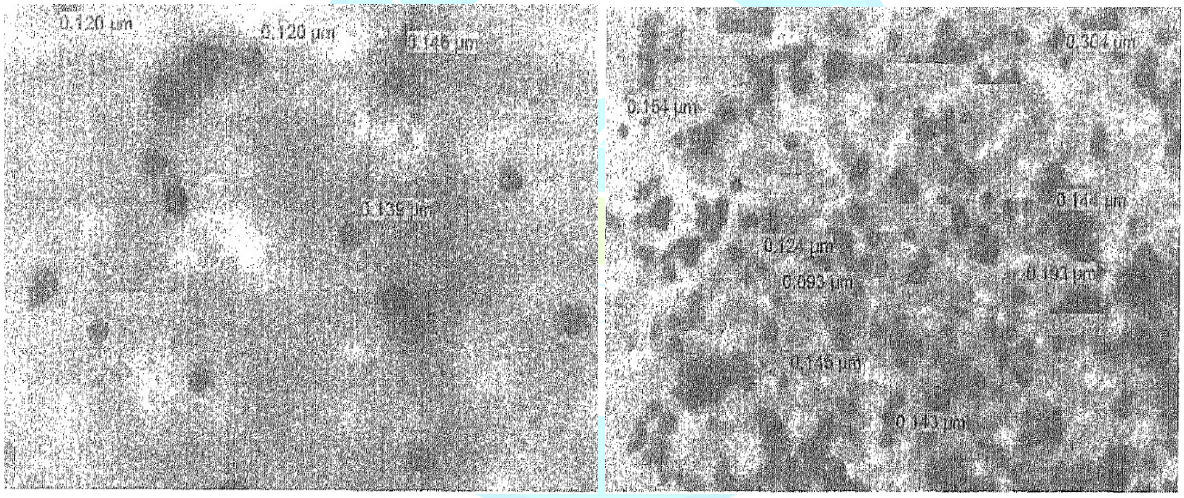

Figure 5-27. TEM images of Paclitaxel loaded stearic acid – SLN (1% w/v poloxamer)

Figure 5-28. TEM images of Paclitaxel loaded stearyl amine – SLN (1% w/v poloxamer)

3.4.3 Differential scanning calorimetry

DSC analysis of paclitaxel-loaded SLNs (stearic acid and stearyl amine) showed no melting peak of paclitaxel at 219.59°C (Figs. 5-3, 5-29, 5-30), indicating that the drug was present in an amorphous form or molecularly dispersed within the SLNs.

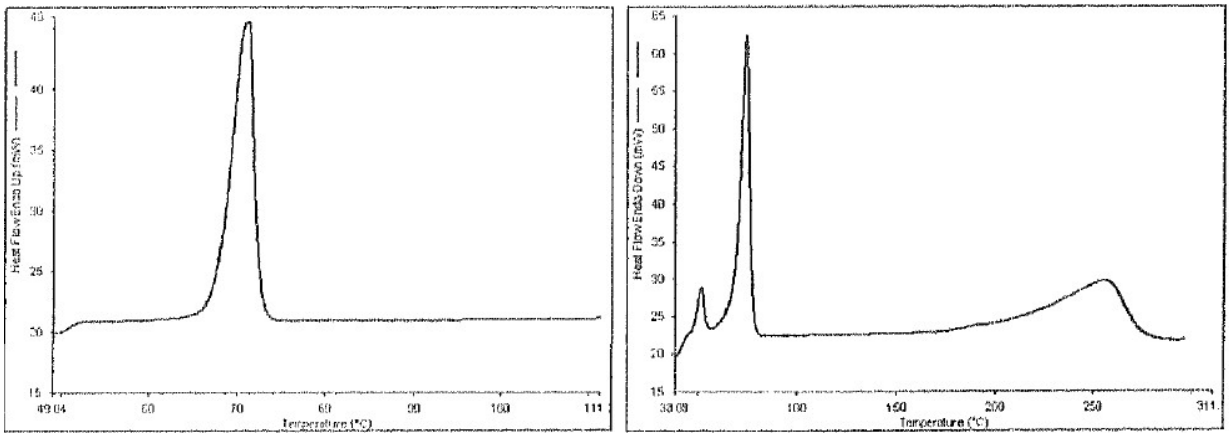

(a) (b)

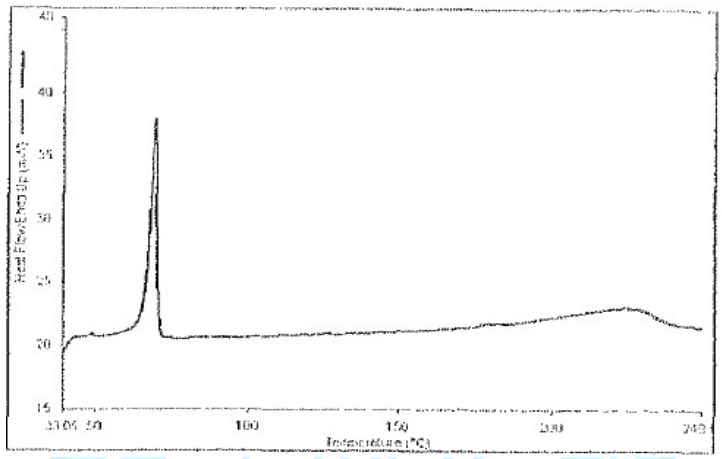

Figure 5-29. DSC thermogram of (a) stearic acid, (b) stearic acid physical mixture, and (c) paclitaxel loaded stearic acid-SJLN

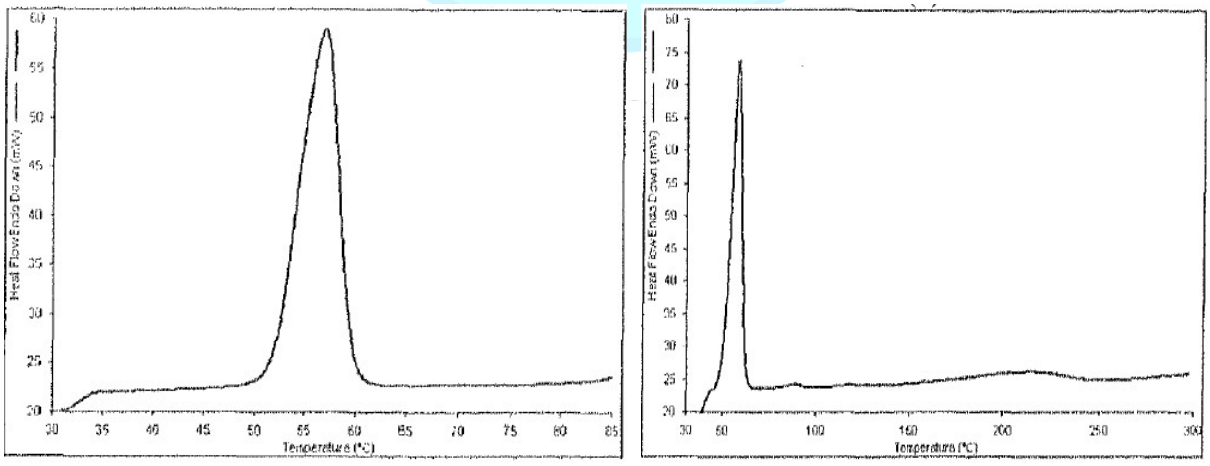

(a) (b)

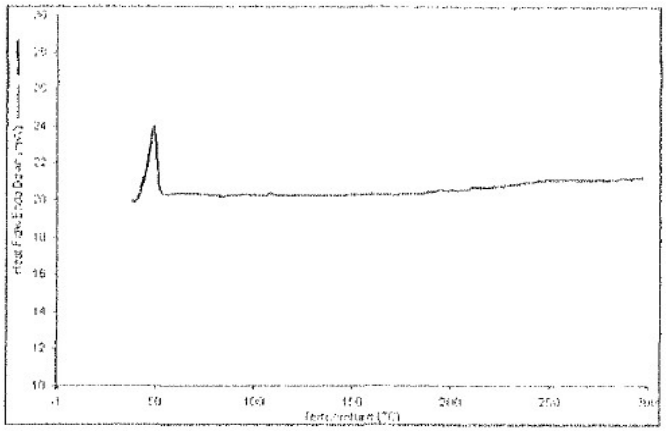

(c)

Figure 5-30. DSC thermogram of (a) stearyl amine, (b) stearyl amine physical mixture, and (c) paclitaxel loaded stearyl amine-SLN

3.4.4 Surface Chemistry characterization

FTIR analysis showed that poloxamer coated the SLN surface, as indicated by characteristic peaks (3500, 2884, 1114 cm^{-1}). Paclitaxel peaks were largely absent, confirming it was mostly encapsulated within the lipid core. Minimal drug was present on the surface due to its low water solubility.

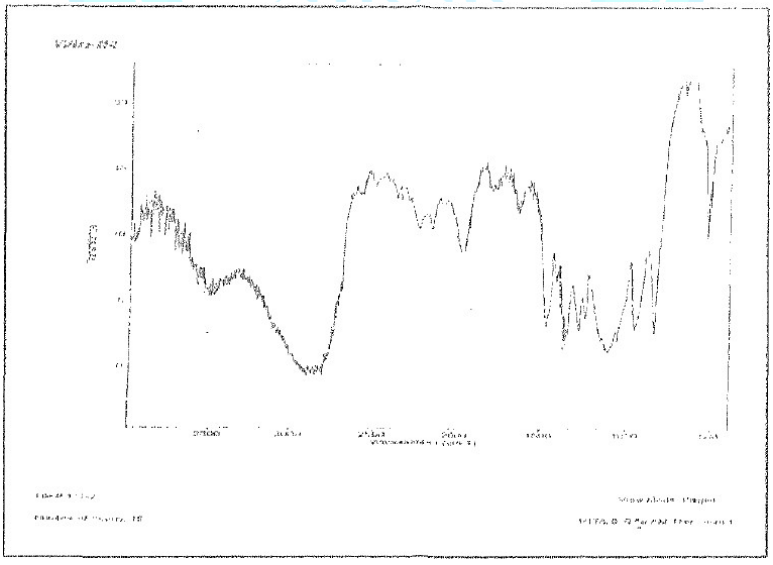

Fig 5-33. FTIR Spectra of Poloxamer 188

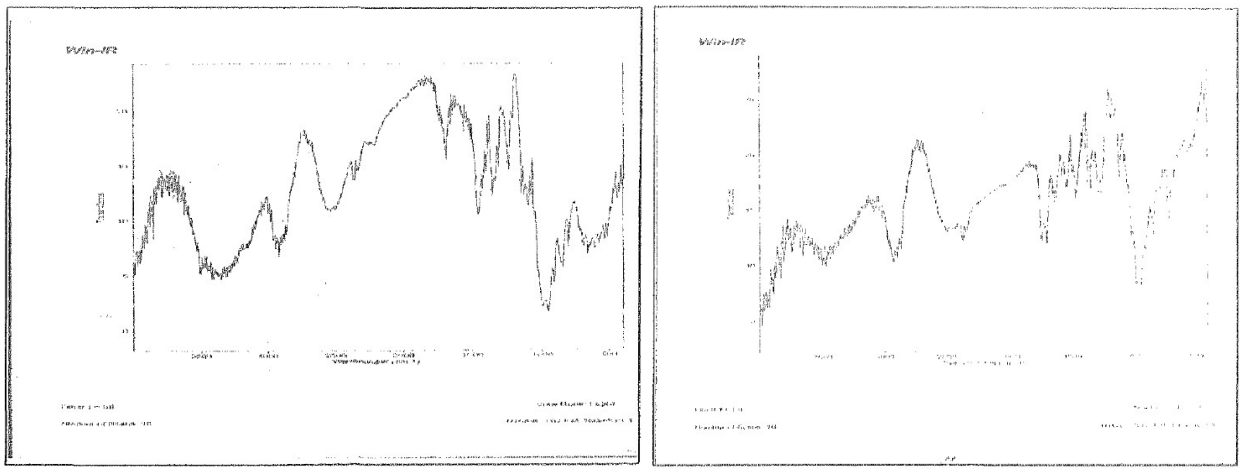

(a) (b)

Fig 5-34. FTIR spectra of (a) drug free steric acid-SLN, (b) paclitaxel-loaded steric-acid-SLN

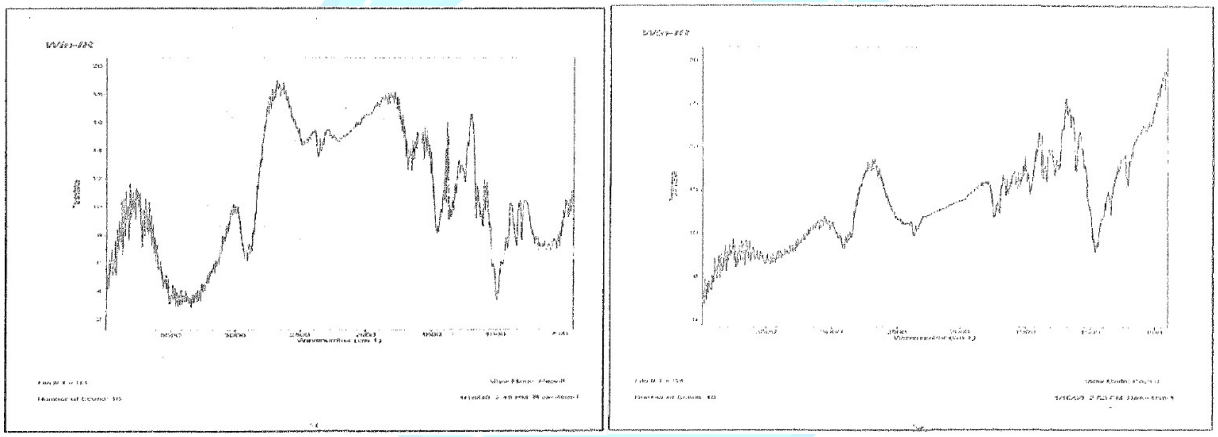

(a) (b)

Fig 5-35. FTIR spectra of (a) drug free stearylamine-SLN, (b) paclitaxel-loaded stearylamine-SLN

3.5 STAIBILITY STUDIES OF OPTIMIZED PACLITAXEL LOADED SLN

The stability of paclitaxel-loaded SLNs is critical for reproducibility and in vivo performance, as lipid systems are prone to physical instability (aggregation, fusion) and chemical degradation (oxidation, hydrolysis). To mitigate these effects, α-tocopherol was included as an antioxidant, and SLNs were stored under controlled conditions. Physical and chemical stability was

evaluated at 4°C ± 2°C, 25°C ± 2°C/60% ± 5% RH, and 40°C ± 2°C/75% ± 5% RH over time, using particle size, morphology, zeta potential, drug content, as indicators.

Particle size and shape

Particle size and shape of paclitaxel-loaded SLNs remained stable at 4°C ± 2°C and 25°C ± 2°C/60% ± 5% RH for up to 90 and 60 days, respectively. At 40°C ± 2°C/75% ± 5% RH, a significant increase in particle size was observed after 15 days, likely due to temperature-dependent aggregation, as confirmed by TEM images (Fig. 5-40 to 5-42).

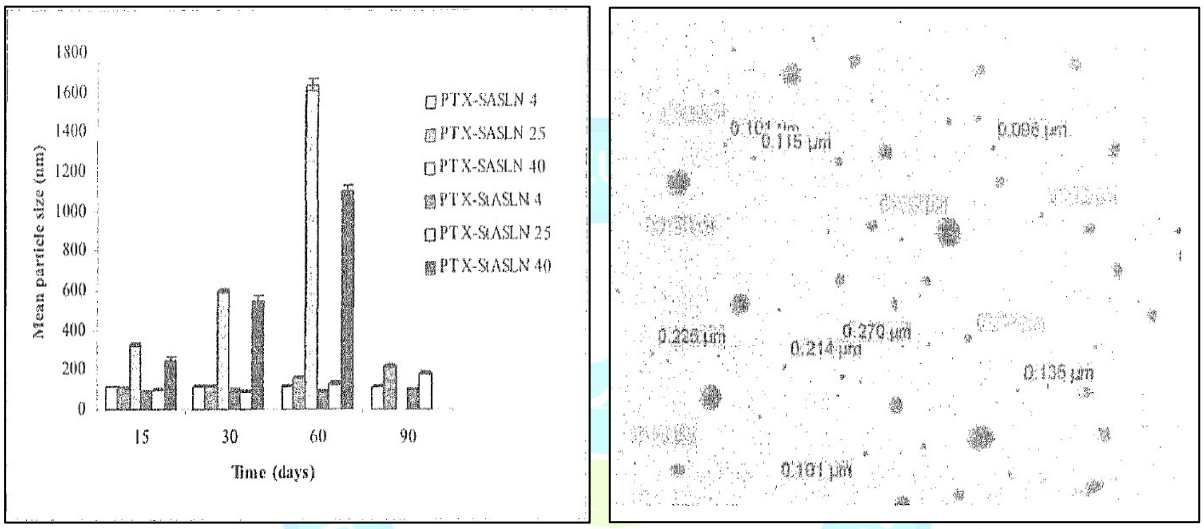

Figure 5-40. Effect of storage conditions on particle size of PTX-SASLN and PTX-StASLN formulations (mean ±SD; n = 3)

Figure 5-41. TEM photomicrograph of the paclitaxel loaded stearylamine SLN formulation at 4°C ± 2°C after 90 days of storage

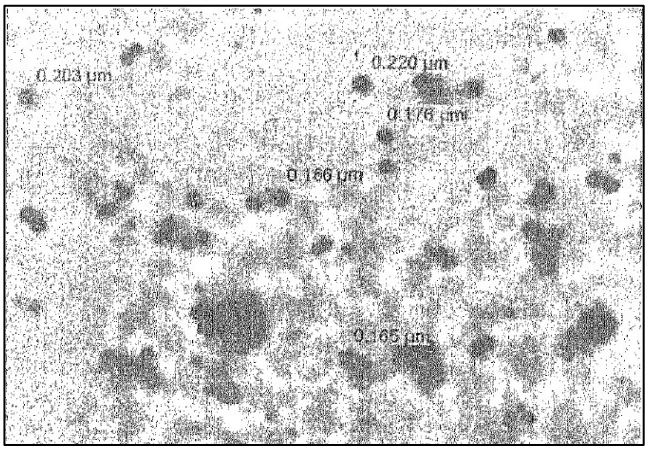

Figure 5-42. TEM photomicrograph of the paclitaxel loaded stearylamine SLN formulation at 40“C ± *2°C/75%* ± 5% RH after 15 days of storage

Zeta Potential

The zeta potential of paclitaxel-loaded SLNs remained stable at 4°C ± 2°C and 25°C ± 2°C/60% ± 5% RH for up to 90 and 60 days, respectively. At 40°C ± 2°C/75% ± 5% RH, zeta potential gradually decreased over 90 days, likely due to gradual loss of the poloxamer coating, reducing steric stability and increasing aggregation risk (Fig. 5-43).

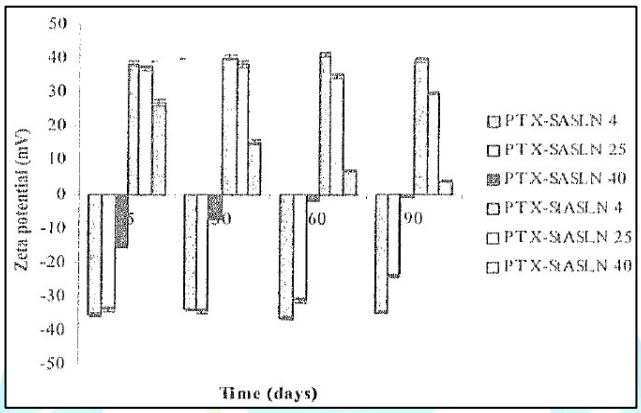

Figure 5-43. Effect of storage conditions on zeta potential of PTX-SASLN and PTX-StASLN formulations (mean ± SD; n=3)

Residual Drug Content

Paclitaxel-loaded SLNs retained >99.99% of drug at 4°C ± 2°C for 90 days. At 25°C ± 2°C/60% ± 5% RH, 50–60% of the drug remained after 90 days, whereas at 40°C ± 2°C/75% ± 5% RH, only ~8–10% was retained after 30 days (Fig. 5-44). Logarithmic plots of % drug remaining versus time are shown in Fig. 5-45.

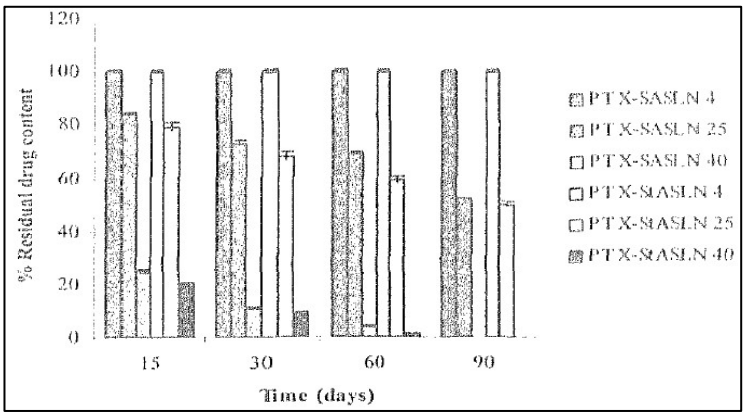

Figure 5-44. Effect of storage conditions on the percentage of residual drug content, of PTX-SASLN and PTX-StASLN formulations (mean ± SD; n=3)

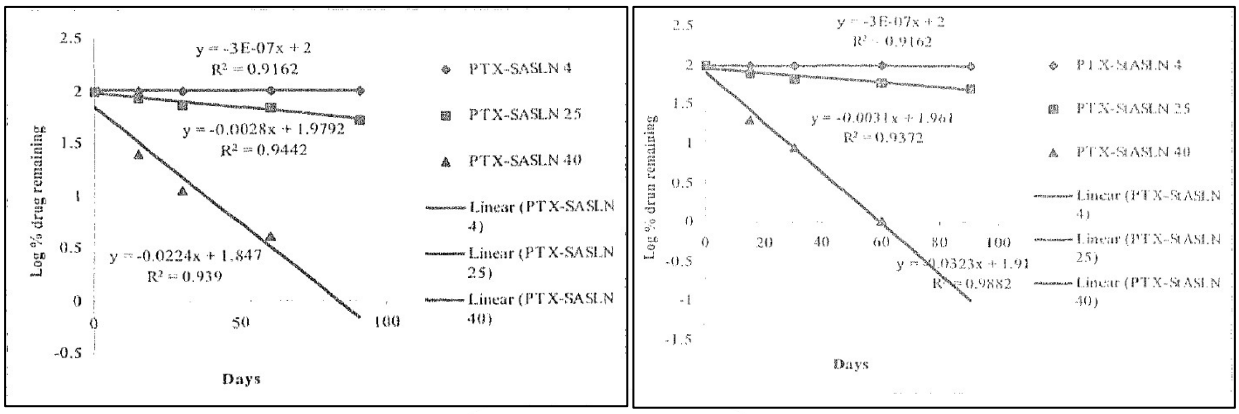

(c) (b)

Figure 5-45. Plot of log % drug remaining and time for optimized paclitaxel loaded SLN formulations of (a) stearic acid, and (b) stearylamine

3.6 *IN VIVO* STUDIES

These studies evaluated the in vivo plasma concentrations and organ distribution of orally administered paclitaxel-loaded SLN. Results showed that the SLN system was orally absorbed, maintained sustained plasma drug levels, and exhibited measurable uptake in organs including the liver, spleen, lungs, brain, and kidney, providing insights for improved oral paclitaxel delivery.

3.6.1 Plasma Profiles

Plasma profiles were analyzed using non-compartmental pharmacokinetics. After oral administration, Cmax values for free paclitaxel and paclitaxel-SLN were 3087 ± 424 ng/mL and 10,274 ± 1875 ng/mL, respectively, while i.v. free paclitaxel reached 7887 ± 617 ng/mL. Oral SLN administration showed delayed clearance and ~10-fold higher plasma levels than free drug, indicating that poloxamer-coated SLN improved circulation time, protected paclitaxel from enzymatic and chemical degradation, and significantly enhanced oral bioavailability (AUC).

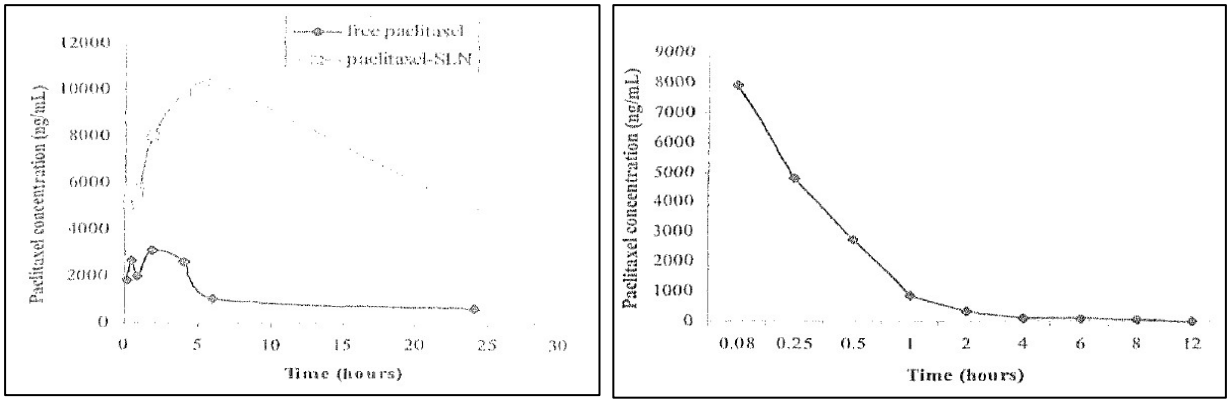

(d) (b)

Figure 5-47. Plasma concentration time profile of paclitaxel in mice with (a) (orally administered free paclitaxel and paclitaxel-SLN formulation, (b) intravenously administered free paclitaxel

Table 5-12. Pharmacokinetic parameters of paclitaxel in different formulations obtained from in vivo studies in mice*.

Route	**i.v.**	**Oral**	
Formulation	**Free Paclitaxel**	**Free Paclitaxel**	**Paclitaxel-SLN**
Dose (mg/kg)	10	40	40
Pharmacokinetic parameters			
C_{max} (ng/ml)	7887	3087	10274
t_{max} (h)	-	2.0	6.0
$t_{1/2}$ (h)	2.29	10.75	22.46
AUC_{0-t} (ng.h)/ml	4666	28887	185218
AUC_{0-inf} (ng.h)/ml	4666	29161	187307
CL_T (L/h/kg)	2.14	-	-

*Pharmacokinetic parameters calculated by non-compartmental model. All data is mean n=5.

Table 5-13. Comparative concentration* time profiles of paclitaxel in mice (oral) with free paclitaxel and paclitaxel-SLN formulation

Time (hours)	**0.25**	**0.5**	**1**	**2**	**4**	**6**	**24**

Free paclitaxel	1836±296	2648±3.04	1975±337	3087±424	2593±545	1050±402	626±145
PaclitaxelSLN	5044±756	5741±995	5592±985	7981±988	9920±1384	10274±1875	4784±593

*Concentration in ng/ml

Group	$AUC_{0\text{-}inf}$ (ng.hr)/ml	Dose (mg/kg)	Bioavailability (%)
Free paclitaxel (oral)	29161	40	1.6
Paclitaxel-SLN (oral)	187307	10	10.0
Free paclitaxel (i.v.)	4666	10	-

3.6.2 Tissue Distribution Profiles

Tissue distribution profiles (Fig. 5-48) showed that oral paclitaxel-SLN achieved ~2-fold higher concentrations in tissues than free paclitaxel (Table 5-15). Maximum concentrations in liver, lungs, kidney, spleen, and brain for free paclitaxel vs. paclitaxel-SLN were 5627 ± 859 vs. 6973 ± 254; 8378 ± 1234 vs. 3786 ± 704; 3889 ± 529 vs. 4713 ± 709; 3561 ± 684 vs. 4672 ± 538; and 3851 ± 726 vs. 7565 ± 678 ng/g, respectively. Tissue exposure indicated systemic absorption, with liver distribution suggesting a first-pass effect, which was lower for SLN than free paclitaxel.

Table 5-15. Comparative exposure (AUC ng.hr/g) of paclitaxel in various tissues of mice after oral administration of free paclitaxel and paclitaxel-SLN formulation

Tissue	Area under curve of tissue concentration time profile		
	Free paclitaxel (A)	Paclitaxel-SLN (B)	Fold (A/B)
Liver	69272	127694	2
Lung	86565	76091	1
Kidney	58637	100889	2
Spleen	43275	91736	2
Brain	77894	171985	2

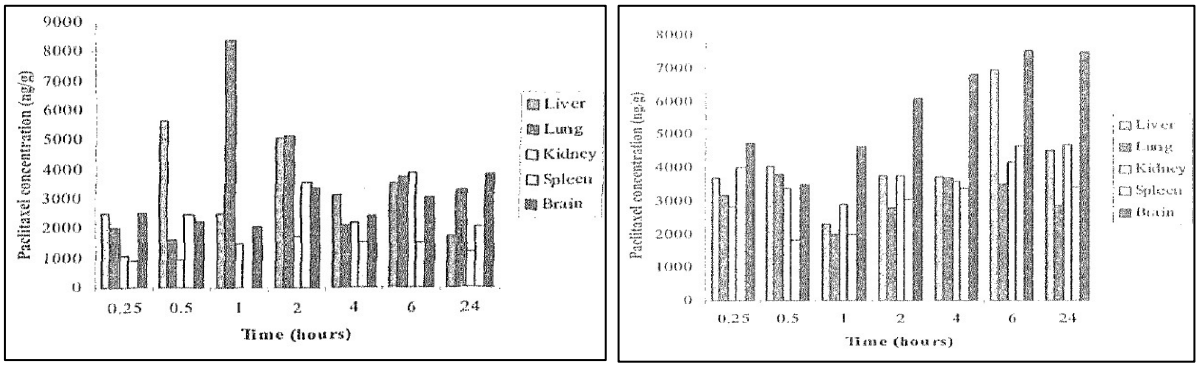

(a) (b)

Figure 5-48. Tissue concentration time profiles of paclitaxel after oral administration of (a) free paclitaxel, and (b) paclitaxel-SLN formulation

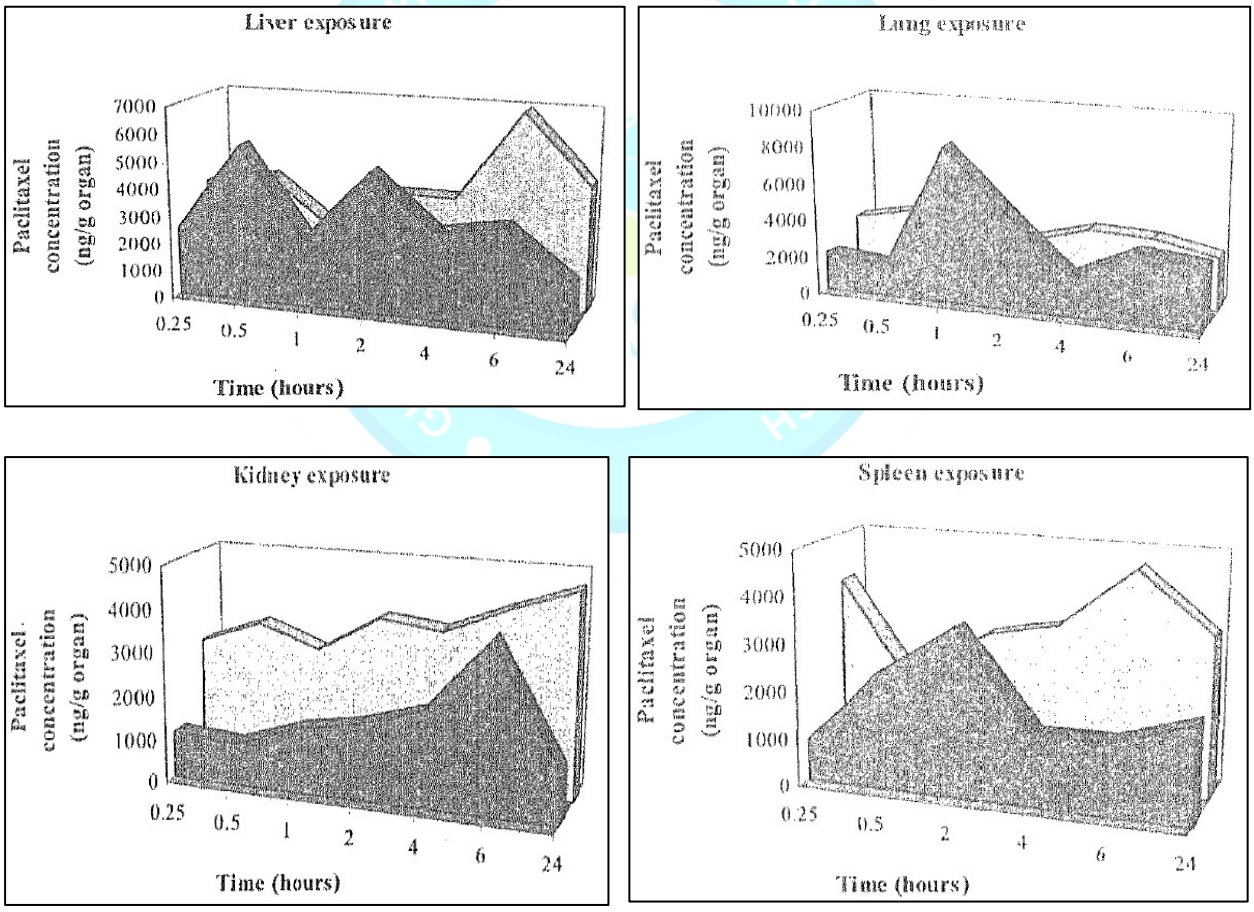

(c) (d)

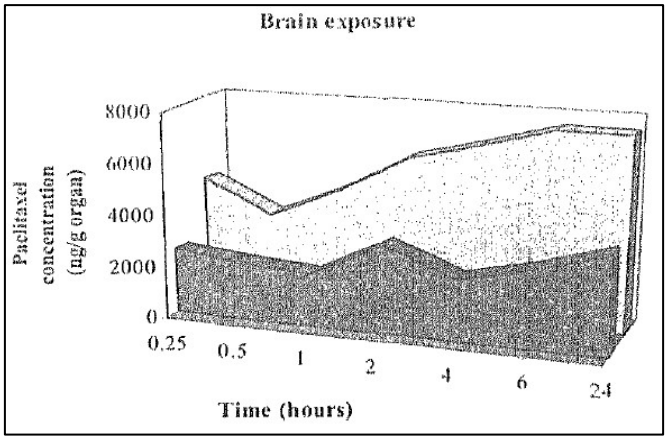

(e)

Figure 5-49. Comparative paclitaxel exposure after oral administration of free paclitaxel and paclitaxel-SLN formulation in (a) liver, (b) lung, (c) kidney, (d) spleen and, (e) brain

Conclusion: After oral administration, paclitaxel-SLN achieved 10-fold higher plasma and 2-fold higher tissue exposure compared to free paclitaxel. One-way ANOVA ($F = 29.024$, $p = 0.000$) confirmed that the differences in plasma concentration-time profiles were statistically significant (Table 5-16). These results demonstrate that SLN significantly enhanced the oral bioavailability of paclitaxel by protecting the drug from gastrointestinal degradation, prolonging transit time, and facilitating translocation across epithelial barriers.

Table 5-16. Anova single factor analysis

Source of variation	Df	SS	MS	F	P-value
Between Treatments	1	90124388.643	90124388.64	29.024	0.000
Residual	12	37261975.714	3105164.643		
Total	13	127386364.357			

4. Conclusion

This study demonstrates that optimized paclitaxel-loaded solid lipid nanoparticles can effectively overcome the major limitations of oral paclitaxel delivery. The modified solvent injection technique produced stable, uniformly sized nanoparticles with high drug

incorporation, amorphous drug dispersion, and favorable surface characteristics. These formulations significantly enhanced oral bioavailability, achieving ~10-fold higher plasma exposure and greater tissue uptake than free paclitaxel, while maintaining excellent safety in toxicity evaluations. Together, the findings confirm that SLNs provide a promising, biocompatible, and efficient platform for oral paclitaxel administration and hold potential for developing safer, non-invasive chemotherapeutic therapies.

5. Acknowledgment

We express our sincere gratitude to Institution for providing the necessary facilities and resources to conduct this research. We are also grateful to our colleagues and laboratory staff for their assistance in experimental procedures and data analysis.

6. Conflict of Interest

The authors declare no conflict of interest related to this research.

7. References

- Bancroft, W. D. (1913). The theory of emulsification. *Journal of Physical Chemistry*, *17*, 501–519.
- Batzri, S., & Korn, E. D. (1973). Single bilayer liposomes prepared without sonication. *Biochimica et Biophysica Acta (BBA) – Biomembranes*, *298*(4), 1015–1019.
- Bocca, C., Gasco, M. R., & Gallarate, M. (1998). Solid lipid nanoparticles for oral drug delivery. *Journal of Controlled Release*, *52*(1–2), 27–35.
- Cavalli, R., Gasco, M. R., & Chetoni, P. (2000). Preparation and characterization of solid lipid nanoparticles (SLN). *Journal of Microencapsulation*, *17*(6), 751–760.
- Chen, Y., Chai, L., & Li, J. (2001). HPLC method for determination of paclitaxel in biological samples. *Journal of Chromatography B: Biomedical Sciences and Applications*, *758*, 235–241.
- Dhanikula, A. B., & Panchagnula, R. (2004). Characterization of paclitaxel-loaded chitosan microspheres. *International Journal of Pharmaceutics*, *281*(1–2), 97–113.
- Freitas, C., & Müller, R. H. (1999). Effect of storage and surface coating on the physical stability of solid lipid nanoparticles (SLN). *International Journal of Pharmaceutics*, *182*(1), 97–105.

- Gasco, M. R. (1997). Preparation of solid lipid nanoparticles (SLN) using microemulsion technique. *Drug Development and Industrial Pharmacy*, *23*(12), 1233–1245.
- Goymann, C., & Schubert, R. (2003). Solvent injection technique for lipid nanoparticle preparation. *International Journal of Pharmaceutics*, *258*(1–2), 123–131.
- Heydenreich, R., Müller, R. H., & Mäder, K. (2003). Characterization of SLN: Particle size, morphology, and zeta potential. *Pharmaceutical Research*, *20*(9), 1455–1461.
- Hirota, M. (1998). In vitro evaluation of drug release from nanoparticles. *Journal of Controlled Release*, *54*(2), 85–93.
- Holmberg, K. (1998). *Surfactants and polymers in aqueous solutions*. John Wiley & Sons.
- Lee, K. D., Kim, J. H., & Choi, H. K. (1999). Paclitaxel quantification in plasma by HPLC. *Journal of Pharmaceutical and Biomedical Analysis*, *19*(5), 789–795.
- Lee, M. K., Kim, M. Y., Choi, J. W., & others. (2007). Preparation, characterization and in vitro cytotoxicity of paclitaxel-loaded sterically stabilized solid lipid nanoparticles. *Biomaterials*, *28*(12), 2137–2146.